Journal of Photochemistry, 3 (1974/75) 71 - 87

INFRA-RED LASER ENHANCED REACTIONS: CHEMISTRY OF VIBRATIONALLY EXCITED O_3 WITH NO AND $O_2(^1\Delta)$*

MICHAEL J. KURYLO and WALTER BRAUN
Physical Chemistry Division,

ANDREW KALDOR and SAMUEL M. FREUND
Optical Physics Division, National Bureau of Standards, Washington, D.C. 20234 (U.S.A.)

RICHARD P. WAYNE
Physical Chemistry Laboratory, Oxford University, Oxford OX1 3QZ (Gt. Britain)

(Received November 14, 1973; in revised form December 6, 1973)

Summary

Vibrationally excited ozone, produced by absorption of CO_2 laser radiation, was found to react significantly faster with NO and $O_2(^1\Delta)$ than thermal ozone. Using a modulation technique, absolute and relative rate constants at 300K for the following reactions were calculated assuming rapid equilibration between the three closely spaced vibrationally excited levels of O_3, and that only the lowest level of these, the ν_2 bending mode, is active in reaction.

$$O_3 + NO \rightarrow NO_2^*(^2B_1) + O_2 \quad (1)$$
$$O_3^\dagger + NO \rightarrow NO_2^*(^2B_1) + O_2 \quad (1')$$

$$O_3 + NO \rightarrow NO_2^\dagger(^2A_1) + O_2 \quad (2)$$
$$O_3^\dagger + NO \rightarrow NO_2^\dagger(^2A_1) + O_2 \quad (2')$$

$$O_3 + O_2(^1\Delta) \rightarrow 2O_2 + O \quad (7)$$
$$O_3^\dagger + O_2(^1\Delta) \rightarrow 2O_2 + O \quad (7')$$

$k_{1'} + k_{2'} = 2.7 \times 10^{-13}$ cm^3 molecule^{-1} s^{-1}; $(k_{1'} + k_{2'})/(k_1 + k_2) = 16.2 \pm 4.0$; $k_{1'}/k_1 = 4.1 \pm 2.0$; $k_{2'}/k_2 = 17.1 \pm 4.3$; $k_{7'}/k_7 = 38 \pm 20$. These rate constants must be modified if a different combination of vibrationally excited levels is involved. The fraction of vibrational energy usable in chemical reaction was found to be about 15, 50 and ~ 100% respectively for processes 1′, 2′ and 7′. Our measurements clearly differentiate between the participation of vibrational energy and thermal energy but do not distinguish differences between the individual vibrationally excited states. Details of the modulation technique, involving chemiluminescence detection of NO_2 and resonance fluorescence detection of oxygen atoms, are described. Comparison of our results with a previous measurement of the summation reaction (1′ + 2′) shows excellent agreement.

* Work supported in part by Climatic Impact Assessment Program, Department of Transportation, Office of Secretary, and Measures for Air Quality Program, NBS, Washington, D.C.

Introduction

Rate constants for reactions involving simple species, *e. g.* atoms plus diatomic or triatomic molecules or diatomics plus diatomic or triatomic molecules are usually measured as Maxwell–Boltzmann averages. Such rate measurements are performed under bulk or bath conditions and the resulting rate constants are dependent only on ambient gas temperature. There has long been interest in and speculation about the effect of excess internal reactant energy on the measured rate constant for chemical reactions. Extensive experimental evidence indicates that products resulting from the reaction of atoms with simple diatomic molecules frequently possess considerable excess internal energy [1 - 3]. Detailed energy balance arguments (*i. e.* the principle of microscopic reversibility) would therefore predict that the reverse reaction(s), involving reactants with excess internal energy would proceed significantly faster than with reactants where the internal energy has a Maxwell–Boltzmann distribution corresponding to the bath temperature. This conclusion is supported by a variety of experimental and theoretical results from the laboratories of Polanyi [4], Bauer [5], and others [6]. Vibrational and rotational energy in simple diatomics can electronically excite Na [7, 8]. Recently, vibrationally excited OH (v=2 to v=9) has been shown to react with ozone and other diatomic and triatomic molecules at significantly higher rates than does thermalized OH [9].

With the advent of lasers and the ability to tune them to specific molecular absorptions, it has now become possible to investigate specific reaction processes involving vibrationally excited species. Odiorne *et al.* [10] employed a molecular beam technique to show a two order of magnitude enhancement of the reaction rate of K with HCl upon laser excitation of the HCl. Bauer *et al.* [11] have recently been able to influence the rate of gas phase H_2–D_2 metathesis by specific vibrational excitation. Still more recent measurements by Gordon and Lin (GL) [12] have shown conclusively that NO reacts with vibrationally excited O_3 at least one order of magnitude faster than with ground state or thermal O_3. Finally, a recent flash photolysis study has shown that vibrational excitation in CN radicals produces no changes in the rate constants for the exothermic reaction with O atoms to produce CO but can possibly enhance the rate of the endothermic channel which produces NO [13].

We describe here several experiments in which 9.6 μm radiation from a CO_2 laser was used to produce vibrationally excited O_3, (001). Details are given of an apparatus and procedure which employ both chemiluminescence and resonance fluorescence to monitor the effect of this excess vibrational energy on the rate constants for the reactions $O_3^\dagger + NO \rightarrow NO_2 + O_2$ and $O_3^\dagger + O_2(^1\Delta) \rightarrow 2O_2 + O(^3P)$. We evaluate our experimental observations in relation to the participation of the various possible vibrational states.

Previous measurements on the $O_3^\dagger$ + NO system by GL using a Q switched CO_2 laser tuned to the P(12) transition are re-examined here using a different experimental method and different experimental conditions.

Our objectives are two-fold. As part of more extensive studies designed to measure other reactions of vibrationally excited ozone we employ the NO + $O_3^\dagger$ reaction as a calibrant. (This procedure is described later in the paper.) We therefore need to establish a more precise value for the rate constant for the NO + $O_3^\dagger$ reaction. The modulation method employed here has higher signal to noise than the pulse method employed by GL for equivalent power levels and allows for a more precise rate constant determination [23]. Secondly, the increased sensitivity enables us to extend the earlier measurements to very dilute ozone and NO concentrations and very low steady state laser power levels. While our modulation method is more sensitive for measuring decay processes, it has the disadvantage of being unable to unravel any very short lived phenomena ($\tau < 30$ μs). Nevertheless this modulation method complements the Q switched pulsed experiments and yields somewhat different information on this rather complex chemical system.

Experimental

A (1 m) CO_2 laser, tunable to specific rotational lines in the 9.6 and 10.4 μm region, was employed in the following experiments; the wavelength was determined by a CO_2 spectrum analyzer.

Measurements of the absorption of CO_2 laser radiation by ozone indicated that the strongest coincidence was with the P(30) (9.6 μm) line (1043 cm^{-1}) and the majority of experiments were performed using this transition. Precise absorption data at the P(30) line were obtained using a long path (50 cm) cell containing O_3 and O_2 together with a differential power measurement technique. Ozone concentrations (here and in later experiments) were determined by measuring its absorption of 253.7 nm radiation (emitted from a low pressure mercury arc lamp and isolated through a narrow band interference filter). The CO_2 laser, tuned to the peak gain for the P(30) line, was operated in continuous wave mode with an average output power of 3 - 4 W. The laser power was periodically checked with a disc calorimeter and was monitored continuously using a pyroelectric detector. Experiments were performed with real-time detection techniques in a modulated mode. The CO_2 laser was square-wave chopped by focusing the output of the laser to a point at the chopper wheel using a 10 cm focal length NaCl lens. The chopped beam was then defocused into the experimental apparatus. Because of optical losses, the laser power entering the active cell region was typically 0.6 W. Chopping frequencies could be continuously varied from 0 Hz to 2000 Hz. The chopped waveform of the laser source was monitored at the exit of the apparatus using a pyroelectric detector and the phasing, transmitted power, and modulation frequency could thus be continuously determined. Details of the complete experimental apparatus are shown schematically in Fig. 1. The multi-purpose reaction cell, equipped with NaCl capped laser entrance and exit ports, the gas inlets, ports for the atom-monitoring resonance lamp, and fluorescence (chemiluminescence) monitoring photomultiplier tubes is

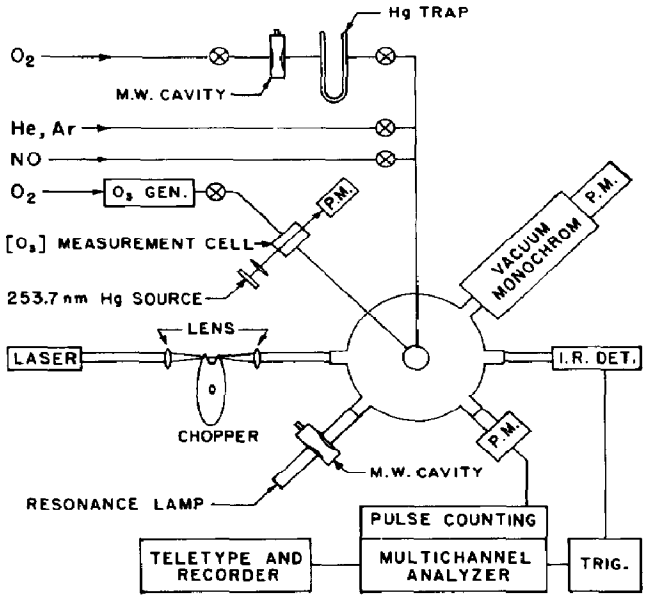

Fig. 1. Schematic diagram of apparatus. PM represents any of the photomultipliers used.

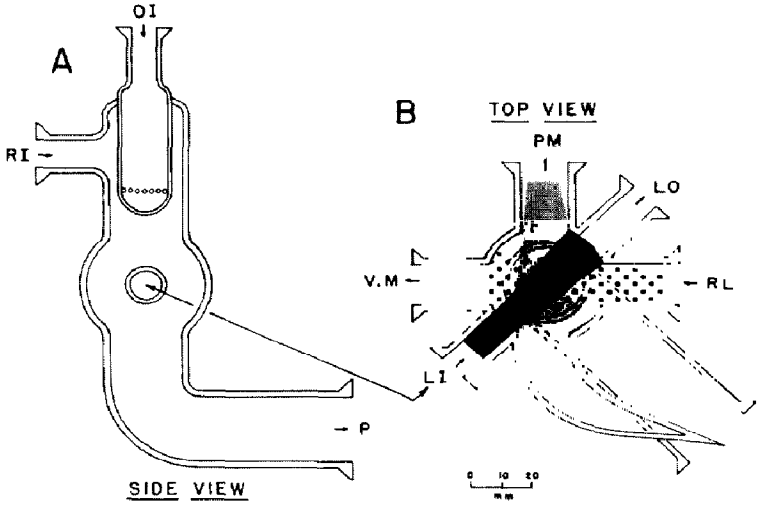

Fig. 2. (A) Side view of reaction cell. RI, reactant inlet; OI, ozone inlet; P, pump. Some side ports are not shown. (B) Top view of reaction cell. LI, laser in; VM, vacuum monochromator; PM, photomultiplier; LO, laser out; RL, resonance lamp. The projections indicate the photomultiplier viewing zone, and the laser and resonance lamp illuminating zones.

shown in detail in Fig. 2. Exact cell geometry and dimensions are indicated since subsequent calculations depend on them.

Experiments were performed under fast flow conditions. A 7 l/s mechanical pump provided residence times of less than 1 ms for gases traversing the

laser and detection zone ($\sim$ 1 cm). In order to minimize heating effects a residence time in the cell of the order of the lifetime of vibrationally excited O_3 (V–T transfer) was considered important. To facilitate performing a large number of experiments under such fast flow conditions it was deemed desirable to use O_3 directly from an ozone generator and accept the presence of O_2. Ozone was thus prepared continuously by a silent discharge in O_2 at atmospheric pressure in a commercial ozonizer. The exit $O_3 + O_2$ stream could be bled into the reaction cell through a needle valve and the concentration of O_3 continuously monitored either at the cell entrance or at the intersection of the laser beam. Pressures of O_2 in the cell were typically 0.5 - 4 Torr, with an O_3 level about 4% of this. Pressures were measured, within a few mTorr, with a digital-capacitance differential manometer.

Two different detection techniques were used. Rates of the reaction of vibrationally excited O_3 with NO were measured using the visible chemiluminescent radiation from electronically excited NO_2, NO_2^*, produced *via* one channel of the reaction, [14, 15]. A photomultiplier was employed for this purpose. Data were acquired using pulse amplifiers and multiscaling. A multichannel analyzer was synchronized to the chopped laser output with known phase relationship. For this purpose the analyzer was triggered by the amplified output of the i.r. detector located at the cell's laser exit port. The waveform of the exciting laser beam could itself be recorded by converting the amplified i.r. detector voltage to frequency. The resulting waveform could then be displayed on the multichannel analyzer. The production of oxygen atoms from reaction of $O_2(^1\Delta)$ with vibrationally excited ozone was measured using resonance fluorescence detection. Vacuum u.v. radiation resonantly scattered by O atoms is detected at 90° to an atomic oxygen resonance lamp [16]. A solar blind vacuum u.v. photomultiplier viewed this fluorescence through the same collimating section used for the NO_2^* chemiluminescence measurements. The oxygen atom ($\sim$ 130.3 nm) radiation was freed from Lyman α (121.6 nm) radiation by a CaF_2 window on the photomultiplier port. Signals were again processed using pulse counting and multiscaling techniques.

All gases were used directly from cylinders and were of ultra high purity grade (O_2, He, Ar). Reagent grade nitric oxide was found by mass spectrometric analysis to be better than 99% pure. Oxygen, $O_2(^1\Delta)$, was prepared using conventional techniques [17] by a microwave discharge in a low pressure (0.5 Torr) flow of O_2. Oxygen atoms were effectively eliminated from the reaction cell by passing the discharged gas through a mercury mirrored trap. The effectiveness of O atom removal could be ascertained by monitoring O atom resonance fluorescence in the reaction cell. Upon addition of O_3 to the $O_2(^1\Delta)$ stream the production of O atoms from the reaction $O_2(^1\Delta) + O_3 \rightarrow O + 2O_2$ provided sufficient evidence for the presence of $O_2(^1\Delta)$ [18 - 20]. Since absolute concentrations of $O_2(^1\Delta)$ were not required, monitoring [21, 22] of $O_2(^1\Delta_g)$ was not deemed necessary.

Procedure

The reaction between ozone and NO proceeds through two parallel channels. The first, reaction (1), produces electronically excited NO_2; the second, reaction (2), produces NO_2 in its ground electronic state.

$$O_3 + NO \xrightarrow{k_1} NO_2^*(^2B_1) + O_2 \quad (1)$$

$$O_3 + NO \xrightarrow{k_2} NO_2^\dagger(^2A_1) + O_2 \quad (2)$$

The rate constant for reaction (1), $k_1 = 1.27 \times 10^{-12} \exp(-4200/RT)$ cm^3 $molecule^{-1}$ s^{-1} is roughly ten times less than the rate constant for reaction (2), $k_2 = 7.17 \times 10^{-13} \exp(-2300/RT)$ cm^3 $molecule^{-1}$ s^{-1} at 298 K [14, 15]. If we initially assume the existence of a single vibrationally excited state, the following equations dictate the enhanced production of NO_2^* due to $O_3^\dagger$:

$$O_3 + \text{laser} \xrightarrow{\Phi(t)} O_3^\dagger \quad (3)$$

$$O_3^\dagger + NO \xrightarrow{k_1'} NO_2^* + O_2 \quad (1')$$

$$O_3^\dagger + NO \xrightarrow{k_2'} NO_2^\dagger + O_2 \quad (2')$$

$$O_3^\dagger + M \xrightarrow{k_4} O_3 + M \quad (4)$$

$$NO_2^* + M \xrightarrow{k_5} NO_2 + M \quad (5)$$

$$NO_2^* \xrightarrow{k_6} NO_2 + h\nu \quad (6)$$

In reaction (3), $\Phi(t)$ represents the pumping rate, photons absorbed cm^{-3} s^{-1}, and is a constant value when the laser is on and zero when the laser is off. Kinetic equations based on the series of reactions can be solved for the total time dependence of $[O_3^\dagger]$. However, for the sake of simplicity we have restricted our analysis to the "laser off" period during which $[O_3^\dagger]$ is given by:

$$[O_3^\dagger] = [O_3^\dagger]_{max} \exp(-\lambda_1 t) \quad (I)$$

where $[O_3^\dagger]_{max}$ is the $O_3^\dagger$ concentration at the moment the laser turns off and t is the elapsed time which equals zero when the laser turns off and $1/(2f)$ when the laser turns back on, (f being equal to the chopping frequency). λ_1 is given by:

$$\lambda_1 = (k_1' + k_2')[NO] + k_4[M] + k_p \quad (II)$$

where k_p is associated with removal of $O_3^\dagger$ by mechanical pumping and M refers to any deactivating gas. In the present work we monitor the NO_2^* emission *via* process (6), which follows the NO_2^* concentration. Over this same "laser off" period the modulated part of the NO_2^* concentration is given by:

$$[NO_2^*] = (\lambda_1/(\lambda_2 - \lambda_1))[O_3^\dagger]_{max}[\exp(-\lambda_1 t) - \exp(-\lambda_2 t)] + [NO_2^*]_0 \exp(-\lambda_2 t) \quad (III)$$

$$\text{where } \lambda_2 = k_5[M] + k_6 + k_p \quad (IV)$$

$[NO_2^*]_0$ is the concentration of NO_2^* in the viewing zone at the moment the laser turns off, and t is defined as for eq. (I). Since λ_2 has a value many times larger than λ_1, ($\tau_2 = 1/\lambda_2 < 1\ \mu s$) [24] eq. (III) reduces to:

$$[NO_2^*] = A \exp(-\lambda_1 t) \tag{V}$$

for $\Delta t \leqslant t \leqslant 1/2f$. We employ this equation in our analysis as the decay of the visible chemiluminescence parallels the decay of $[O_3^\dagger]$. Experimental conditions were usually chosen to minimize deactivation of $O_3^\dagger$ (reaction 4), although, at very low concentrations of NO, the influence of deactivation and removal by mechanical pumping (k_p) can be detected.

The time dependent portion of the NO_2^* emission is added to a steady state emission due to reaction (1). We therefore performed a non-linear least squares analysis of the decay curves using the functional form:

$$I = I_0 \exp(-\lambda_1 t) + I_{ss} \tag{VI}$$

where I_{ss} is the steady state emission intensity. The determination of λ_1 leads to a value for $(k_1' + k_2')$. Separate experiments in which the peak NO_2^* modulation was determined at low chopping frequencies established k_1'/k_1. These are described in the discussion of eqn. (X).

For the reaction of $O_2(^1\Delta)$ with vibrationally excited ozone:

$$O_3^\dagger + O_2(^1\Delta) \xrightarrow{k_7'} 2O_2 + O \tag{7'}$$

an expression for O atom production can be derived which corresponds exactly with eqn. (III). There is a notable difference, however, between the analyses of the NO + $O_3^\dagger$ data and the $O_2(^1\Delta)$ + $O_3^\dagger$ data. In the former case, decay data reflect the occurrence of chemical reaction. In the latter case, both the concentrations of $O_2(^1\Delta)$ and $O_3^\dagger$ are so low that the decay rate reflects only $O_3^\dagger$ deactivation and/or the rate at which both $O_3^\dagger$ and oxygen atoms are physically removed from (pumped out of) the apparatus viewing zone. The rate constant for process (7') must therefore be determined not by measuring the variation with time of the oxygen atom concentration, but by measuring the depth of modulation. In the square-wave (low chopping frequency) limit the modulation can be determined from a steady-state analysis of the following rate processes:

$$O_3 \xrightarrow{\Phi(t)} O_3^\dagger \tag{3}$$

$$O_3^\dagger + M \xrightarrow{k_4} O_3 + M \tag{4}$$

$$O_3^\dagger \xrightarrow{k_p} \text{removal through pumping}$$

$$O_3 + O_2(^1\Delta) \xrightarrow{k_7'} 2O_2 + O \tag{7}$$

$$O_3^\dagger + O_2(^1\Delta) \xrightarrow{k_7} 2O_2 + O \tag{7'}$$

$$O \xrightarrow{k_p} \text{removal through pumping}$$

With the laser off, the steady state concentration of O atoms in the viewing zone is derived from:

$$d[O]/dt = k_7[O_2(^1\Delta)]\ [O_3]_0 - k_p[O]\ + F = 0 \qquad \text{(VII)}$$

When the laser is on, we obtain:

$$d[O]/dt = k_7[O_2(^1\Delta)]\ ([O_3]_0 - [O_3{}^\dagger]) + k_7'[O_2{}^1\Delta]\ [O_3{}^\dagger] - - k_p[O]\ + F = 0 \qquad \text{(VIII)}$$

The term F (in units of molecule cm^{-3} s^{-1}) represents any influx of atoms into the viewing zone from the reaction of $O_3 + O_2(^1\Delta)$ directly above the viewing zone. $[O_3]_0$ is the ozone concentration during the laser-off period.

Solving eqns. (VII) and (VIII) for [O] we obtain:

$$[O]_{on}/[O]_{off} = \frac{k_7[O_2(^1\Delta)]\ ([O_3]_0 - [O_3{}^\dagger]) + k_7'[O_2(^1\Delta)]\ [O_3{}^\dagger]\ + F}{k_7[O_2(^1\Delta)]\ [O_3]_0 + F} \qquad \text{(IX)}$$

Extraction of (k_7'/k_7) requires a value for $[O_3{}^\dagger]/[O_3]$. To obtain this, a small amount of NO was added in each of the $O_2(^1\Delta) + O_3$ experiments and the $NO_2{}^*$ modulation signal was measured. $[O_3{}^\dagger]/[O_3]$ can then be calculated from the steady state expression for the square wave modulation in the $NO + O_3{}^\dagger$ experiments

$$[NO_2{}^*]_{on}/[NO_2{}^*]_{off} = \frac{k_1([O_3]_0 - [O_3{}^\dagger]) + k_1'[O_3{}^\dagger]}{k_1[O_3]_0} \qquad \text{(X)}$$

once a value for (k_1'/k_1) is known. Here there is no term resembling the function F.

The ratio (k_1'/k_1) was determined separately as follows. A laser power absorption measurement (long pass cell with our usual operating pressures) was made to determine $\Phi(t)$. From this we calculate:

$$([O_3{}^\dagger]/[O_3])_{NO} = \Phi(t)/(k_p + k_4[M]) \qquad \text{(X')}$$

where the average lifetime, $1/(k_p + k_4[M])$ was measured in an actual experiment with little NO present. The validity of eqn. (X') was tested by varying the lifetime by adding a deactivating gas. A three-fold variation of the lifetime was paralleled by a decrease in the modulation signal to one-third.

The values of $([O_3{}^\dagger]/[O_3])_{NO}$ thus obtained have to be corrected by a geometric factor (see Fig. 2) which takes into account the fact that the phototube views reaction (chemiluminescence) over a volume element larger than that irradiated by the laser. Careful analysis of the conical intersections involved (projections in Fig. 2) indicate a downward correction of 1.8 ± 0.2. We can then recalculate effective values for $([O_3{}^\dagger]/[O_3])_{NO}$ under specified pressure conditions of the chemiluminescent experiments.

The analysis up to now has been based on a simple one-level model assuming involvement of only one vibrationally excited ozone level, $O_3{}^\dagger$, and ground state ozone, O_3. In reality, three vibrationally excited ozone states,

TABLE 1

Ozone Fundamental Vibrational Modes

	Designation	$\epsilon_i(cm^{-1})$	$\exp(-\epsilon_o/kt)$*	$\exp(+\epsilon_o/kt)$†	Relative populations at 298 K
ν_1	Symmetric stretch	1110	0.0048	208.5	1.00
ν_2	Bend	705	0.0337	29.7	7.02
ν_3	Antisymmetric stretch	1043	0.0067	148.4	1.40

* Fractional population at 298 K.

† Maximum theoretical rate constant enhancement due to given mode based solely on energy considerations at 298 K.

representing the three fundamental vibrational modes, must be considered (Table 1). In the present experiments, the CO_2 laser was tuned to the ν_3 anti-symmetric stretch mode which, as seen in Table 1, is nearly degenerate with the symmetric stretch ($\Delta E \sim -67\ cm^{-1}$), and energetically somewhat more removed from the ν_2 bending mode ($\Delta E \sim 338\ cm^{-1}$). Since all of these levels are approximately within kT of one another one would have to assume rapid equilibration between them. Depending on which level(s) are involved in chemical reaction, our simplified reaction scheme must be suitably modified. In pulse measurements GL have clearly observed a fast induction period in the NO_2^* fluorescence following laser excitation of the ν_3 mode. Our modulation experiments, as previously mentioned, are insensitive to detection of a rapid build-up followed by a significantly slower decay. Based on their measurements, GL concluded that the pumped level, ν_3, is not involved in the chemical reaction. A model based on two vibrationally excited levels of ozone was therefore considered and is reproduced here.

If the pumped state, $O_3^\dagger$, can equilibrate rapidly with a second vibrationally excited O_3 state, $O_3^\dagger$, and only the second state, $O_3^\dagger$, can react with NO, the previous scheme must be modified by the following reactions:

$$O_3 + \text{laser} \xrightarrow{\Phi(t)} O_3^\dagger \tag{3'}$$

$$O_3^\ddagger + M \xrightarrow{k_{4'}} O_3 + M \tag{4'}$$

$$O_3^\ddagger + M \underset{k_{-8}}{\overset{k_8}{\rightleftharpoons}} O_3^\dagger + M \tag{8}$$

If equilibration, through reaction (8), is very rapid, two limiting cases can be considered: (i) if the equilibrium constant $K = [O_3^\dagger]/[O_3^\ddagger]$ is much greater than unity, essentially all of the $O_3^\ddagger$ produced by the laser is converted over to $O_3^\dagger$ at very short time and the previously derived expression for λ_1, eqn. (II), still applies. If, however, (ii) $K \ll 1$, the classical reactive intermediate case, $[O_3^\dagger]$ is always much smaller than $[O_3^\ddagger]$ and λ_1 now reduces to:

$$\lambda_1 = (k_{1'} + k_{2'})(K)[NO] + k_4K[M] + k_{4'}[M] + k_p \tag{XI}$$

For all values of K, λ_1 can be solved, in closed form.

$$\lambda_1 = \frac{1}{2}\{B + k_8 + k_{-8} + k_{4'} - [(B - k_8 + k_{-8} - k_{4'})^2 + 4k_8k_{-8}]^{1/2}\} \quad \text{(XII)}$$

where $B = (k_{1'} + k_{2'})[\mathrm{NO}] + k_4[\mathrm{M}] + k_p$, and [M] has been absorbed into the values for k_8 and k_{-8}. The steady state expressions, eqns. (IX) and (X), must also be modified if rapid equilibration between two or more vibrationally excited ozone levels occurs. The quantity $[O_3^\dagger]$ obtained from laser power measurement must be reduced according to the equilibrium fractional population of the actual reacting excited state.

A detailed analysis of the rise and decay times for NO_2^* fluorescence enabled GL on the basis of the simple two level model, to show that the bending mode, ν_2, is active in chemical reaction rather than the symmetric stretch ν_1. The pumped, ν_3, mode was eliminated from the mere evidence of an induction period.

Assuming ν_2 to be the active mode in our experiments, we therefore multiply the geometrically corrected ratios for $([O_3^\dagger]/[O_3])_{NO}$ by 0.745 (*i. e.* ~ 7/9.4, the ratio of ν_2 population to total population given in Table 1).

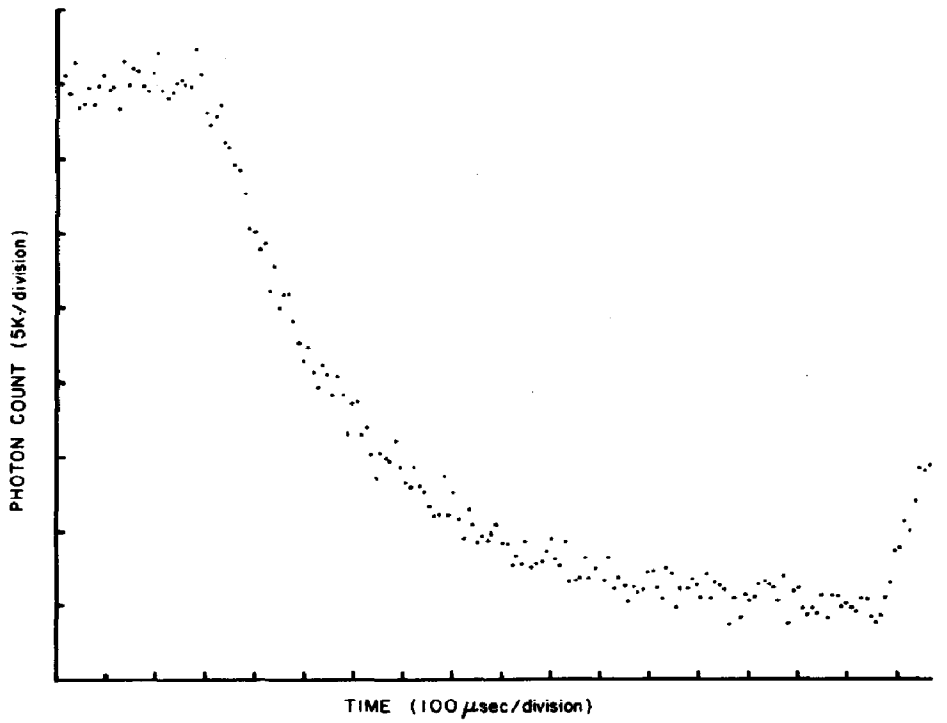

Fig. 3. Typical modulation in an NO + O_3 experiment showing exponential decay of the chemiluminescence attributable to NO + $O_3^\dagger$. P_{Ar} = 4 Torr; P_{O_2} = 2.5 Torr; P_{O_3} = 13 mTorr; P_{NO} = 150 mTorr.

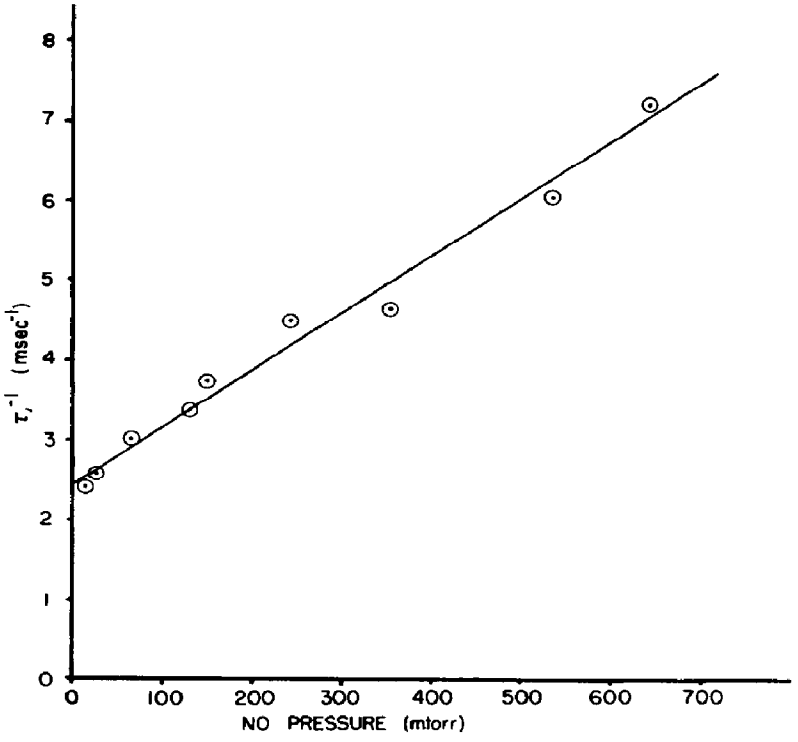

Fig. 4. Plot of first order decay rate ($\lambda_1 = \tau_1^{-1}$) *vs.* NO concentration.

Results

A typical multichannel analyzer display (showing the decay portion of an NO + $O_3^\dagger$ modulation curve) is shown in Fig. 3. As indicated earlier, the rate constant analysis involved non-linear least squares treatment of this fall-off (laser-off) portion of the curve. Experiments performed with the P(30) laser line yielded rate data from which λ_1 [eqns. (I) and (II)] could be determined with a precision of better than 5%. Careful analysis of the residuals showed no evidence for any deviation from a single, simple exponential decay. Values of λ_1 for an individual curve were constant, independent of the portion of the decay curve analyzed (analyses starting anywhere from 30 to 150 μs – 3 to 15 analyzer channels – after the laser cut off. Because of the finite size of the laser beam in the chopper, it took from 1 to 2 channels for the laser intensity to decay completely).

Under the experimental and analysis conditions of the present experiments, no evidence for an induction period in the decay could be detected (for $f \leqslant 1$ kHz). Higher chopping frequencies gave signal levels too weak to be analyzed. Modulation, at the higher frequencies, fell off linearly with f ($f > 300$ Hz) and the phase shift approached 90° in the limit of very high f. (The possible errors in the use of eqn. (II) due to an equilibration of vibrational states, *i. e.* very short induction period, has been discussed. The implications of reducing our data *via* eqn. (XII) are investigated in the discussion section.)

TABLE 2

Rate Data for the NO + $O_3^\dagger$ Reaction

P_{O_3}* (mTorr)	$P_{NO}^\dagger$ (mTorr)	λ_1 (s^{-1})
55	14	2400
38	28	2580
23	67	3000
13	132	3360
13	153	3720
8	244	4470
6	355	4600
5	539	6010
3	646	7150

* This is the average O_3 concentration in the laser irradiated zone during the laser-off period in the presence of the indicated amounts of NO. All runs contain 4 Torr of Ar and 2.5 Torr of O_2.

† These NO pressures have been corrected to account for removal of NO by O_3 upstream of the viewing zone. This was accomplished by subtracting the change in O_3 concentration (when NO was added) from the differentially measured initial NO pressure (concentration).

Since the NO concentration was always at least one order of magnitude lower than the inert gas concentrations (O_2 and Ar) the dependence of λ_1 on [NO] was through reactions (1′) and (2′) and to a good approximation does not involve reaction (4). Thus a plot of λ_1 *vs.* [NO] should yield a straight line with slope ($k_1' + k_2'$) and intercept $k_4[M] + k_p$. Such a plot is shown in Fig. 4. A linear least squares analysis of the data (presented in Table 2) gives: $(k_1' + k_2') + (2.2 = 0.1) \times 10^{-13}$ cm^3 $molecule^{-1}$ s^{-1} where the uncertainty corresponds to one standard deviation. At very low total pressures, and in the limit of zero NO concentration, the decay reflects solely the mechanical pumping rate. Experiments performed under such conditions gave pumping rates (k_p) of 1400 s^{-1} in good agreement with a value of k_p calculated from the measured pumping speed and the cell cross-sectional area.

A precise measurement of k_p is crucial to the computation of the average temperature rise due to laser heating. It is essential to show that the observed enhancement of the reaction rate is due to vibrationally excited species rather than due to thermal effects. The maximum temperature rise in the present experiments can be calculated from the laser power absorption (0.15% cm^{-1} of 0.6 W at 18 mTorr pressure of O_3 and 1 Torr O_2), residence time ($1/k_p \sim 700$ μs), and the heat capacity of the gases present. For the conditions indicated, a temperature rise of 0.4 K can occur upon complete deactivation of $O_3^\dagger$. Our experiments were performed under conditions of minimum $O_3^\dagger$ deactivation during the mechanical pumping time. Indeed, depths of modulation (square wave limit) were found to be at a maximum in the limit of negligible thermal deactivation (*i. e.* the condition of minimum thermal heating).

TABLE 3

Modulation Results from the $O_2(^1\Delta) + O_3^\dagger$ Reaction and the $NO + O_3^\dagger$ Calibration Reaction

P_{O_2} *	P_{He}	P_{O_3}	Mod ($^1\Delta$) (%)	Mod (NO) (%)	$([O_3^\dagger]/[O_3])_{NO}$	$([O_3^\dagger]/[O_3])_{1_\Delta}{}^\dagger$	$k_7'/k_7{}^\ddagger$
1.0	0.0	0.02	63.38	6.64	0.021 **	0.029	33.8
1.0	2.0	0.02	21.53	2.19	0.0071	0.0098	34.0
1.5	1.5	0.04	23.46	2.06	0.0066	0.0091	39.7
2.0	1.0	0.06	28.14	2.23	0.0072	0.0100	43.2
2.5	0.5	0.08	33.49	2.95	0.0095	0.0132	39.1
2.5	0.5	0.08	33.16	2.95	0.0095	0.0132	38.7

*All pressures are expressed in Torr. All runs contain 0.03 Torr of NO.

** Calculated from laser power absorption measurement (geometrically corrected and assuming ν_2 to be the active mode). From this value we calculate $k_1'/k_1 = 4.1$. From this rate constant ratio we calculate the other values in this column using eqn. (X).

† All values in this column are calculated by multiplying the previous column by (1.8/1.3), the geometric correction ratio (see text).

‡ Calculated using eqn. (IX).

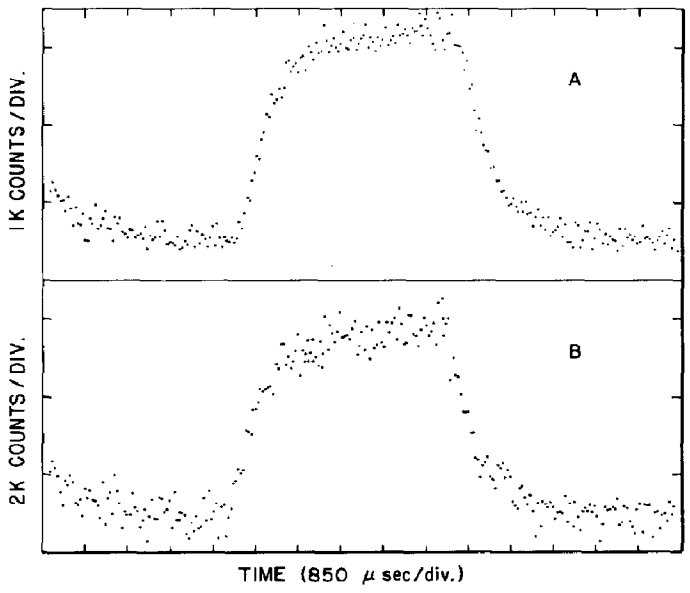

Fig. 5. (A) Modulation of $O_2(^1\Delta) + O_3$ reaction caused by laser excitation of O_3. Viewed by monitoring the O atom product by resonance fluorescence. $P_{O_2} = 1$ Torr $P_{O_3} = 18$ mTorr; $P_{NO} = 30$ mTorr; $P_{O_2}(^1\Delta) = 20$ mTorr (estimated). Total counts = 10.5 K. (B) Modulation of NO + O_3 chemiluminescent calibration reaction under conditions identical to those in (A). Total counts = 102 K.

The results for the modulation experiments on the $O_2(^1\Delta) + O_3^\dagger$ system are shown in Table 3. The percentage modulation values, measured as $([O]_{\text{laser on}} - [O]_{\text{laser off}})/[O]_{\text{laser off}}$, were obtained in the square-wave low frequency limit. Percentage modulation values for NO + $O_3^\dagger$ for similar pressure conditions are also listed since they serve for calibration purposes. Figure 5 shows typical modulation curves for the $O_2(^1\Delta) + O_3^\dagger$ reaction along with the calibration NO + $O_3^\dagger$ curve obtained under identical experimental conditions.

For the first experiment listed, a concentration ratio $([O_3^\dagger]/[O_3])_{NO}$ equal to 0.021 was calculated using the procedure outlined earlier. From eqn. (X) we then calculate $k_1'/k_1 = 4.1 \pm 2.0$ where the uncertainty reflects both the uncertainties in the geometric corrections as well as the modulation measurements. Applying this latter ratio in eqn. (X) we calculate the other values for $([O_3^\dagger]/[O_3])_{NO}$ appearing in the Table. The rate constant ratio can also be used along with our value for $(k_1' + k_2')$ to calculate the rate constant enhancement associated with reactions (2) and (2′) independently. Since $(k_1' + k_2')/(k_1 + k_2) = 13.2$, we find that $k_2'/k_2 = 13.9$ or $k_2' = 2.15 \times 10^{-13}$ cm^3 molecule^{-1} s^{-1}.

If the same geometric correction applied to the resonance fluorescence as to the chemiluminescence measurements, these same concentration ratios could be used to calculate the rate constant enhancements for the reaction of $O_2(^1\Delta) + O_3^\dagger$ (*i. e.* k_7'/k_7) using eqn. (IX). However, analysis of the reso-

nance lamp geometry indicates that it illuminates a volume much smaller than the effective chemiluminescent volume (see Fig. 2). This in turn lowers the geometric correction to a value of 1.3 for the resonance fluorescence experiments. Consequently, for matching pairs of experiments we calculate that $([O_3^\dagger]/[O_3])_{1_\Delta} = (1.8/1.3)([O_3^\dagger]/[O_3])_{NO}$. These values are tabulated in Table 3. Finally, the value for F in eqn. (IX) must be obtained. A simple analysis of cross-sectional areas, flow rates and mixing times indicated that $F = (0.5 \pm 0.5)k_7[O_2(^1\Delta)][O_3]$. Using the mean value we obtain the tabulated values for k_7'/k_7 as calculated from eqn. (IX). Fortunately, the 100% uncertainty in F creates less than 50% uncertainty in k_7'/k_7. We thus obtain an average value for the rate constant enhancement of the $O_2(^1\Delta) + O_3^\dagger$ reaction of 38 ± 20 where the error limit reflects the combined uncertainties of all the measurements and calculations.

Modulations in both the NO and $O_2(^1\Delta)$ systems were found to vary in identical fashions and were determined solely by the influence of deactivation on $[O_3^\dagger]$. As in the NO system, the depth of modulation of the $O_2(^1\Delta)$ reaction was a maximum under conditions of minimum deactivation of $O_3^\dagger$, thus indicating the absence of any heating effects. Measurements performed at different frequencies showed that the modulation depth fell off with increasing frequency faster than that for $NO + O_3^\dagger$. In the high frequency limit, the measured phase shift exceeded 90° as expected since there is a phase shift accompanying both the reaction and the mechanical pumping (O atom removal) process.

Discussion

The simplified data treatment presented in the procedure section was based on a model assuming one excited vibrational level. A modification of this simple model to include two vibrationally excited levels (one of them chemically active) in rapid equilibrium was included. Extension to multiple levels with one or more active modes is possible but not justified in the present work. Without the necessary time resolution, we are unable to distinguish the participation of the various vibrationally excited levels in either the NO or the $O_2(^1\Delta)$ experiments.

According to the analysis of GL, the pumped mode, ν_3, is not active in the NO experiment since they observe an induction period for the NO_2^* chemiluminescence. Further (mathematical) analysis of their results indicated that only the ν_2 bending mode enhances the reaction rate. The induction period can be associated, on the basis of their experiment, only with that channel of the NO reaction producing electronically excited NO_2^* (reaction 1′). Such an induction period may or may not be associated with the non-signal-producing channel (reaction 2′). To include the possibility that reactions (1′) and (2′) involve different vibrational levels would again require a correction procedure similar to that summarized by eqn. (XII). For the simplified analysis, no correction is needed. For the more complex analysis we have assumed, according to GL, participation of only ν_2.

We can thus compare our value for $(k_1' + k_2') = 2.2 \pm 0.1 \times 10^{-13}$ cm^3 molecule^{-1} s^{-1} calculated from eqn. (II) directly with the value of 1.5×10^{-13} cm^3 molecule^{-1} s^{-1} obtained by GL *via* similar analysis. Alternatively, we can correct our value using eqn. (XII) along with values of k_8 and k_{-8} as measured by GL. We thereby obtain $(k_1' + k_2')$ corrected $= 2.7 \pm 0.1 \times 10^{-13}$ cm^3 molecule^{-1} s^{-1} to be compared with a similarly corrected value of $2.5 \pm 0.4 \times 10^{-13}$ cm^3 molecule^{-1} s^{-1} from the work of GL. The agreement, well within the quoted error limits, is quite gratifying in view of the markedly different experimental conditions used in the two studies. Owing to these, the percentage corrections (*via* eqn. XII) ranged from 20%in our case to some 65 % in the higher pressure study of GL.

Our corrected values for $(k_1' + k_2')$ can be used with experimentally measured values of k_1 and k_2 at 298 K to recalculate a corrected value of 16.2 ± 4.0 for $(k_1' + k_2')/(k_1 + k_2)$. This value in turn permits us to obtain a corrected ratio for k_2'/k_2 of 17.1 ± 4.3. There are no results in the literature with which we can compare our individual ratios of k_1'/k_1 and k_2'/k_2.

The tabulation of k_7'/k_7 (Table 3) is based on the assumption that the ν_2 bending mode is, as in the NO + $O_3^\dagger$ system, responsible for the rate constant enhancement. The inclusion of the other modes (ν_1 and ν_3) requires a correction on the term $([O_3^\dagger]/[O_3])_{1_\Delta}$ equal to the ratio of equilibrium concentrations of the various vibrational levels. Thus for involvement of only ν_1 (or ν_3) the enhancement should be multiplied by a factor of about 7 (or 5) (see Table 1).

Within experimental error the enhancement in the reaction rate for the $O_2(^1\Delta)$ + $O_3^\dagger$ reaction is equal to the full Boltzmann factor (Table 1) which means that essentially all of the energy of the vibrational mode is useful in promoting chemical reaction. This is to be compared with the NO + $O_3^\dagger$ system where only about 50% of the energy of vibration is useful for channel (2′), producing ground electronic state NO_2, and about 15% is useful for the channel producing electronically excited NO_2^* (reaction 1′).

Although we have assumed that chemical reaction occurs directly between $O_2(^1\Delta)$ and O_3 we should consider the possibility that the process involves electronic energy transfer, namely:

$$O_3(^1A_1) + O_2(^1\Delta) \rightarrow O_2(^3\Sigma) + O_3(^3A_2) \qquad (9)$$

followed by:

$$O_3(^3A_2) \rightarrow O_2(^3\Sigma) + O(^3P) \qquad (10)$$

Theoretical calculations place the energy of the $^3A_2$ state of O_3 slightly higher than the 0.98 eV energy of $O_2(^1\Delta)$ [25]. The possibility that any vibrational energy in $O_3(^1A_1)$ would promote the energy transfer (process 9) is consistent with the present observation that all the laser excitation energy can be utilized in reaction (7′) and that the activation energy [18] in the thermal reaction roughly equals the endothermicity.

Acknowledgements

The authors wish to gratefully acknowledge the help of Mr. David Rudman and Miss Beverly Chew during various aspects of these experiments. The use of various instrumentation of the NBS Washington Laser Chemistry Project is deeply appreciated.

References

1 J. C. Polanyi, Appl. Optics, 10 (1971) 1717 and references therein.
2 J. H. Parker and G. C. Pimentel, J. Chem. Phys., 51 (1969) 91; 55 (1971) 857 and references therein.
3 T. Carrington and D. Garvin, in Comprehensive Chemical Kinetics, vol. 3, Elsevier, Amsterdam, 1969.
4 K. G. Anlauf, D. H. Maylotte, J. C. Polanyi and R. B. Bernstein, J. Chem. Phys., 51 (1969) 5716; L. J. Kirsch and J. C. Polanyi, ibid., 57 (1972) 4498.
5 A. Lifshitz, C. Lifshitz and S. H. Bauer, J. Am. Chem. Soc., 87 (1965) 143; D. Lewis and S. H. Bauer, ibid., 90 (1968) 5390.
6 S. B. Jaffe and J. B. Anderson, J. Chem. Phys., 49 (1968) 2859.
7 H. F. Krause, J. Fricke and W. L. Fite, ibid., 56 (1972) 4593; J. E. Mentall, H. F. Krause and W. L. Fite, Discuss. Faraday Soc., 44 (1967) 157.
8 D. A. Jennings, W. Braun and H. P. Broida, J. Chem. Phys., 59 (1973) 4305.
9 A. E. Potter, R. N. Coltharp and S. D. Worley, ibid., 54 (1971) 992; R. N. Coltharp, S. D. Worley and A. E. Potter, Appl. Optics, 10 (1971) 1786; S. D. Worley, R. N. Coltharp and A. E. Potter, J. Chem. Phys., 55 (1971) 2608; J. Phys. Chem., 76 (1972) 1511.
10 T. J. Odiorne, P. R. Brooks and J. V. V. Kasper, J. Chem. Phys., 55 (1971) 1980.
11 S. H. Bauer, D. M. Lederman, E. L. Resler and E. R. Fisher, Int. J. Chem. Kinet., 5 (1973) 93.
12 R. J. Gordon and M. C. Lin, Chem. Phys. Lett., 22 (1973) 262.
13 V. H. Schake, K. J. Schmatjko and J. Wolfram, Ber. Buns. Phys. Chem., 77 (1973) 248.
14 M. A. A. Clyne, B. A. Thrush and R. P. Wayne, Trans. Faraday Soc., 60 (1964) 359.
15 P. N. Clough and B. A. Thrush, Chem. Commun., 21 (1966) 783; Trans. Faraday Soc., 63 (1967) 915.
16 D. D. Davis, R. E. Huie, J. T. Herron, M. J. Kurylo and W. Braun, J. Chem. Phys., 56 (1972) 4868.
17 R. P. Wayne, Adv. Photochem., 7 (1969) 311; J. T. Herron and R. E. Huie, J. Chem. Phys., 51 (1969) 4164; R. E. Huie and J. T. Herron, Int. J. Chem. Kinet., 5 (1973) 197.
18 I. D. Clark, I. T. N. Jones and R. P. Wayne, Proc. Roy. Soc., A317 (1970) 407.
19 F. D. Findlay and D. R. Snelling, J. Chem. Phys., 54 (1971) 2750.
20 K. H. Becker, W. Groth and U. Schurath, Chem. Phys. Lett., 14 (1972) 484.
21 L. Elias, E. A. Ogryzlo and H. I. Schiff, Can. J. Chem., 37 (1959) 1680.
22 I. D. Clark and R. P. Wayne, Mol. Phys., 18 (1970) 523.
23 H. E. Hunziker, IBM J. Res. Devel., 15 (1971) 10.
24 G. H. Myers, D. M. Silver and F. Kaufman, J. Chem. Phys., 44 (1966) 718.
25 M. Krauss, personal communication.